



# INITIAL ALIGNMENT OF FIBER-OPTIC INERTIAL NAVIGATION SYSTEM WITH LARGE MISALIGNMENT ANGLES BASED ON GENERALIZED PROPORTIONAL- INTEGRAL-DERIVATIVE FILTER

Mohammad Ali Rahgoshay<sup>1</sup>, Paknoosh Karimaghaie<sup>1</sup>, Fereidoon Shabaninia<sup>1</sup>

School of Electrical & Computer Engineering

Shiraz University, Shiraz

Fars 71345, Iran

Email: [M.rahgoshay@shirazu.ac.ir](mailto:M.rahgoshay@shirazu.ac.ir)

---

*Submitted: May 15, 2017*

*Accepted: July 17, 2017*

*Published: Sep. 1, 2017*

---

*Abstract- Initial alignment in the presence of large misalignment angles is a critical issue in strapdown inertial navigation systems. The large initial misalignment angle adversely affects the accuracy and rapidness of the alignment process. In this paper a novel robust alignment approach is proposed based on a generalized proportional-integral-derivative filter. The proposed alignment approach has some significant advantages compared to the standard Kalman filter based alignment method. This method increases the accuracy and the convergence speed of the alignment process in the large misalignment angles problem. Experimental results also, verify the prominent performance of the presented approach in comparison to conventional standard Kalman filter based alignment method.*

**Index terms:** Standard Kalman Filter, Generalized Proportional-Integral-Derivative Filter, Strapdown Inertial Navigation System, Initial Alignment , Large Misalignment Angles.

## I. INTRODUCTION

Fiber-optic Strapdown Inertial Navigation System (FSINS) is currently among the most prominent and widely used navigation systems in many application fields. Initial alignment is one of the most important steps that must be performed prior to navigation phase of SINS. The aim of initial alignment process is to obtain an accurate estimation of transformation matrix between body frame and computational frame in the shortest possible time [1]. The alignment error is one of the main sources of error in inertial navigation systems so the accuracy of the alignment process directly affects the performance of SINS. The rapidness of the initial alignment procedure is also a determining factor which influences the overall efficiency of the SINS, especially in military applications. The initial alignment procedure itself involves two steps, namely coarse and fine alignments. In coarse alignment step, a rough approximation of transformation matrix is calculated in a very short time. In fine alignment process, the misalignment angles are estimated by using the optimal state estimation theory and subsequently, the transformation matrix is accurately computed.

The Kalman filter (KF) is the most acceptable and useful approach in optimal state estimation theory [2]. In recent decades, the KF has been implemented in many fields of engineering including control, guidance, navigation, etc [3-7]. The standard KF and its extended linear and nonlinear versions are mostly used for initial alignment of SINS. It is also used in aided navigation systems to estimate the unbounded accumulative errors of the inertial navigation system [8-11].

The standard KF-based alignment method utilizes linear dynamics error model of SINS to accomplish estimation process of the misalignment angles. This method assumes that the misalignment angles are small at the beginning of the estimation procedure. However, this assumption depends on the performance of the coarse alignment, and it is not satisfied in some conditions and applications.

The conventional coarse alignment method is based on the supposition that the vehicle is at rest and the inertial sensors only sense the Earth's rotation rate and gravitational acceleration. In marine mooring conditions, the inertial measurement unit (IMU) experiences relatively large random movements and subsequently the coarse alignment accuracy is significantly reduced. A novel coarse alignment algorithm based on the inertial frame was developed to overcome this problem

[12-14]. By using inertial frame based methods, coarse alignment can be performed appropriately in quasi-stationary mooring condition. However, these methods take a relatively long time (about two minutes) to achieve reasonable accuracy and satisfy the small initial misalignment angles assumption for the fine alignment procedure. The concept of in-motion alignment also suffers from the large misalignment angles problem [15-17]. In fact, based on mission operational conditions or as a failure mode, it is sometimes necessary to perform the initial alignment when the vehicle is in motion condition [18]. In this cases, the aforementioned coarse alignment methods cannot be implemented which subsequently leads to the problem of large initial misalignment angles in the initial alignment phase.

In the presence of large initial misalignment angles, the standard KF-based approach does not meet the desired accuracy and rapidness for alignment procedure. In fact, to design optimal estimation procedure, the KF requires accurate knowledge of the system model. Despite the system model uncertainty, standard KF is not an optimal estimator and may even sometimes lead to an unstable filter. Due to the robustness and generality property, the nonlinear filtering and adaptive methods are used in most research to improve the performance of fine alignment with large initial misalignment angles [19-23]. These methods use the nonlinear dynamics error model of SINS which consider the large misalignment angles to obtain appropriate performance in the initial alignment process. Although, each of these alignment methods has its own disadvantages such as computational complexity and implementation burdens.

In 2016, Zhang et al. introduced the concept of Generalized Proportional-Integral-Derivative Filter (GPIDF) based on the Proportional-Integral-Derivative (PID) controller idea [24]. Unlike the KF, the GPIDF employs the past, present and future measurement information to estimate current state vector which leads to a more accurate estimation procedure. According to the intrinsic properties of proportional-integral-derivative controllers, this filter has desirable robustness property compare to the standard KF. Furthermore, unlike the nonlinear and adaptive filtering methods, the GPIDF has a simple structure which leads to the reduction of computational complexity and on-line implementation burdens. In this paper based on the proportional-integral-derivative filter idea, a new alignment approach is presented for marine SINS under mooring conditions with large initial misalignment angles. This new proposed alignment method manifests considerable advantages which improve the performance of the SINS alignment process in the problem of large misalignment angles uncertainty. A performance comparison is performed by

Experimental turntable test to show the superiority of the presented approach to standard KF-based alignment method.

## II. THE STATE AND MEASUREMENT EQUATIONS FOR INERTIAL FRAME BASED ALIGNMENT

In order to implement a filtering algorithm, the state and measurement equations must first be extracted. In the literature, the velocity error and the misalignment angles on the inertial frame are considered as the states of an inertial frame based fine alignment procedure. So, the state equations for SINS alignment on the inertial frame are written as [25]:

$$\delta \dot{\mathbf{V}}^i = -[\mathbf{g}^i(t) \times] \delta \mathbf{V}^i(t) + \mathbf{C}_b^i(t) \mathbf{V}_{bias}^b + \mathbf{C}_b^i(t) \mathbf{V}_{noise}^b \quad (1-1)$$

$$\dot{\boldsymbol{\phi}}^i = -\mathbf{C}_b^i(t) \boldsymbol{\varepsilon}_{bias}^b - \mathbf{C}_b^i(t) \boldsymbol{\varepsilon}_{noise}^b \quad (1-2)$$

In above equations,  $\mathbf{V}_{noise}^b$  and  $\boldsymbol{\varepsilon}_{noise}^b$  are the velocity error and the misalignment angles of Gaussian white noises, respectively.  $\mathbf{V}_{bias}^b$  is the accelerometer bias vector and  $\boldsymbol{\varepsilon}_{bias}^b$  is the gyroscope bias vector and it is supposed that they have Gaussian distribution.  $\mathbf{C}_b^i$  is the transformation matrix from the body frame (b-frame) to the inertial frame (i-frame) which is computed accurately at the end of the alignment process. Finally, the transformation matrix from the b- frame to local-level frame (n-frame) is computed as follows:

$$\mathbf{C}_b^n = \mathbf{C}_i^n \mathbf{C}_b^i \quad (2)$$

Where  $\mathbf{C}_i^n(t)$  is the transformation matrix between the i-frame and the n-frame computed as:

$$\mathbf{C}_i^n(t) = \begin{bmatrix} -\sin l & \cos l & 0 \\ -\sin L \cos l & -\sin L \sin l & \cos L \\ \cos L \cos l & \cos L \sin l & \sin L \end{bmatrix} * \begin{bmatrix} \cos[\omega_{ie}(t-t_0)] & \sin[\omega_{ie}(t-t_0)] & 0 \\ -\sin[\omega_{ie}(t-t_0)] & \cos[\omega_{ie}(t-t_0)] & 0 \\ 0 & 0 & 1 \end{bmatrix} \quad (3)$$

In which,  $\omega_{ie}$ ,  $L$  and  $l$  are the Earth's rate and geographical latitude and longitude of the vehicle, respectively.

The skew-symmetric matrix  $[\mathbf{g}^i(t) \times]$  can be computed by the inertial gravity vector:

$$\mathbf{g}^i = \begin{bmatrix} -g \cos L \cos(\omega_{ie}(t - t_0) + l) \\ -g \cos L \sin(\omega_{ie}(t - t_0) + l) \\ -g \sin L \end{bmatrix} \quad (4)$$

Where  $g$  is the local gravity vector.

The dynamic error equations (1-1) and (1-2) can be represented as following state-space equations:

$$\dot{\mathbf{X}}(t) = \mathbf{A}(t)\mathbf{X}(t) + \mathbf{B}(t)\mathbf{W}$$

$$= \begin{bmatrix} 0_{3 \times 3} & -[\mathbf{g}^i(t) \times] & 0_{3 \times 3} & \mathbf{C}_b^i(t) \\ 0_{3 \times 3} & 0_{3 \times 3} & -\mathbf{C}_b^i(t) & 0_{3 \times 3} \\ 0_{3 \times 3} & 0_{3 \times 3} & 0_{3 \times 3} & 0_{3 \times 3} \\ 0_{3 \times 3} & 0_{3 \times 3} & 0_{3 \times 3} & 0_{3 \times 3} \end{bmatrix} \mathbf{X} + \begin{bmatrix} 0_{3 \times 3} & -[\mathbf{g}^i(t) \times] & 0_{3 \times 3} & \mathbf{C}_b^i(t) \\ 0_{3 \times 3} & 0_{3 \times 3} & -\mathbf{C}_b^i(t) & 0_{3 \times 3} \\ 0_{3 \times 3} & 0_{3 \times 3} & 0_{3 \times 3} & 0_{3 \times 3} \\ 0_{3 \times 3} & 0_{3 \times 3} & 0_{3 \times 3} & 0_{3 \times 3} \end{bmatrix} \begin{bmatrix} [\mathbf{V}_{noise}^b]_{3 \times 1} \\ [\mathbf{V}_{noise}^b]_{3 \times 1} \\ 0_{3 \times 1} \\ 0_{3 \times 1} \end{bmatrix} \quad (5)$$

Where  $\mathbf{X} = \left[ [\delta \mathbf{V}^i]^T \quad [\boldsymbol{\varphi}^i]^T \quad [\boldsymbol{\varepsilon}_{bias}^b]^T \quad [\mathbf{V}_{bias}^b]^T \right]^T$  is the state vector.

The measurement vector is obtained from the difference between the velocity vector calculated from INS algorithm and the true velocity vector in the inertial frame. The measurement equation can be represented as:

$$\mathbf{Y} = \begin{bmatrix} \hat{V}_x^i - V_x^i \\ \hat{V}_y^i - V_y^i \\ \hat{V}_z^i - V_z^i \end{bmatrix} = [I_{3 \times 3} \quad 0_{3 \times 9}] \mathbf{X} + \mathbf{N}_{3 \times 1} \quad (6)$$

Where  $\mathbf{Y}$  is the measurement vector and  $\mathbf{N}$  is the measurement noise.  $\hat{\mathbf{V}}^i$  can be obtained by integrating the projection of the accelerometer's measured specific force ( $\mathbf{f}^b$ ) into the i-frame:

$$\hat{\mathbf{V}}^i(t) = \int_{t_0}^t \mathbf{C}_b^i(t) \mathbf{f}^b dt \quad (7)$$

The  $\mathbf{V}^i$  is a known measurement vector which can be calculated by the integration of the inertial gravity vector from the interval of  $t_0$  to  $t$ .

### III. THE GENERALIZED PROPORTIONAL-INTEGRAL DERIVATIVE FILTER

Consider a linear system with following state equations [24]:

$$\mathbf{x}(\mathbf{k} + 1) = \mathbf{A}\mathbf{x}(\mathbf{k}) + \mathbf{B}\mathbf{u}(\mathbf{k}) + \mathbf{w}(\mathbf{k}) \quad (8-1)$$

$$\mathbf{y}(\mathbf{k}) = \mathbf{C}\mathbf{x}(\mathbf{k}) + \mathbf{D}\mathbf{u}(\mathbf{k}) + \mathbf{v}(\mathbf{k}) \quad (8-2)$$

Where  $\mathbf{x}(\mathbf{k}) \in \mathbb{R}^n$ ,  $\mathbf{u}(\mathbf{k}) \in \mathbb{R}^m$  and  $\mathbf{y}(\mathbf{k}) \in \mathbb{R}^k$  are the system state, control input and measurement, respectively.  $\mathbf{w}(\mathbf{k})$  and  $\mathbf{v}(\mathbf{k})$  represent the process and measurement noises. The matrices  $\mathbf{A}$ ,  $\mathbf{B}$ ,  $\mathbf{C}$  and  $\mathbf{D}$  represent the system model and have appropriate dimensions.

The structure of a Generalized Proportional-Integral-Derivative Filter is defined as equations (9) to (18):

$$\hat{\mathbf{x}}(\mathbf{0}|\mathbf{0}) = \bar{\mathbf{x}}_0 \quad (9)$$

$$\mathbf{x}_I(0) = \mathbf{0} \quad (10)$$

$$\tilde{\mathbf{y}}(0) - \tilde{\mathbf{y}}(-1) = \mathbf{0} \quad (11)$$

$$\tilde{\mathbf{y}}(\mathbf{k}) = \mathbf{y}(\mathbf{k}) - \mathbf{C}\hat{\mathbf{x}}(\mathbf{k}|\mathbf{k}) - \mathbf{D}\mathbf{u}(\mathbf{k}) \quad (12)$$

$$\hat{\mathbf{x}}(\mathbf{k}|\mathbf{k} - 1) = \mathbf{A}\hat{\mathbf{x}}(\mathbf{k} - 1|\mathbf{k} - 1) + \mathbf{B}\mathbf{u}(\mathbf{k} - 1) \quad (13)$$

$$\mathbf{r}(\mathbf{k}) = \mathbf{y}(\mathbf{k}) - \mathbf{C}\hat{\mathbf{x}}(\mathbf{k}|\mathbf{k} - 1) - \mathbf{D}\mathbf{u}(\mathbf{k}) \quad (14)$$

$$\mathbf{x}_P(\mathbf{k}) = \mathbf{K}_P(\mathbf{k})\mathbf{r}(\mathbf{k}) \quad (15)$$

$$\mathbf{x}_I(\mathbf{k}) = \mathbf{x}_I(\mathbf{k} - 1) + \mathbf{K}_I(\mathbf{k})\tilde{\mathbf{y}}(\mathbf{k} - 1) \quad (16)$$

$$\mathbf{x}_D(\mathbf{k}) = \mathbf{K}_D(\mathbf{k})(\tilde{\mathbf{y}}(\mathbf{k} - 1) - \tilde{\mathbf{y}}(\mathbf{k} - 2)) \quad (17)$$

$$\hat{\mathbf{x}}(k|k) = \hat{\mathbf{x}}(k|k-1) + \mathbf{x}_P(k) + \mathbf{x}_I(k) + \mathbf{x}_D(k) \quad (18)$$

Where  $\mathbf{K}_P$ ,  $\mathbf{K}_I$  and  $\mathbf{K}_D$  are proportional, integral and derivative gains, respectively. Also,  $\mathbf{x}_P$ ,  $\mathbf{x}_I$  and  $\mathbf{x}_D$  are proportional, integral and derivative parts of the estimator respectively. It can be simply shown that when the integral gain and the derivative gain are zero, the GPIDF is converted to a standard Kalman filter. It can be demonstrated that if the following condition is satisfied, the proportional-integral-derivative filter is an optimal filter and satisfies the Minimum Mean Square Error (MMSE) criterion [24]:

$$\begin{bmatrix} \Lambda_{NN^T}(k) & \Lambda_{NM^T}(k) & \Lambda_{NU^T}(k) \\ \Lambda_{NM^T}(k) & \Lambda_{MM^T}(k) & \Lambda_{MU^T}(k) \\ \Lambda_{NU^T}(k) & \Lambda_{MU^T}(k) & \Lambda_{UU^T}(k) \end{bmatrix} \times \begin{bmatrix} \mathbf{K}_P(k)^T \\ \mathbf{K}_I(k)^T \\ \mathbf{K}_D(k)^T \end{bmatrix} + \begin{bmatrix} \Lambda_{LN^T}(k)^T \\ \Lambda_{LM^T}(k)^T \\ \Lambda_{LU^T}(k)^T \end{bmatrix} = \mathbf{0} \quad (19)$$

Where  $\Lambda_{ij^T}(k) = \mathbb{E}\{\mathbf{i}(k)\mathbf{j}(k)^T\}$  and  $L(k)$ ,  $M(k)$ ,  $N(k)$ ,  $U(k)$  are the linear combination of initial estimation error vector, the process noise vectors  $\mathbf{w}(0)$ ,  $\mathbf{w}(1)$ , ...  $\mathbf{w}(k)$  and the measurement noise vectors  $\mathbf{v}(0)$ ,  $\mathbf{v}(1)$ , ...  $\mathbf{v}(k)$  and can be calculated by the system model.

When the derivative gain is zero ( $\mathbf{K}_D = \mathbf{0}$ ), a Strong Robust Proportional-Integral Filter (SRPIF) with a recursive and simple structure is obtained as follows:

$$\mathbf{P}(0|0) = \mathbf{P}_0 \quad (20)$$

$$\mathbf{P}(k|k-1) = \mathbf{A}\mathbf{P}(k-1|k-1)\mathbf{A}^T + \mathbf{W}(k-1) \quad (21)$$

$$\mathbf{R}(k) = \mathbf{C}\mathbf{P}(k|k-1)\mathbf{C}^T + \mathbf{V}(k) \quad (22)$$

$$\mathbf{K}_P(k) = \mathbf{P}(k|k-1)\mathbf{C}^T\mathbf{R}(k)^{-1} \quad (23)$$

$$\mathbf{K}_I(k) = \mathbf{K}_P(k) \quad (24)$$

$$\mathbf{P}(k|k) = (\mathbf{I} - \mathbf{K}_P(k)\mathbf{C})\mathbf{P}(k|k-1) \quad (25)$$

$$\hat{\mathbf{x}}(k|k) = \hat{\mathbf{x}}(k|k-1) + \mathbf{x}_P(k) + \mathbf{x}_I(k) \quad (26)$$

Where  $\mathbf{x}_P$  and  $\mathbf{x}_I$  are computed from equations (14), (15) and (16). This proportional-integral filter has a recursive and simple structure for online implementation.

According to the properties of the GPID filter, this filtering method can be useful to the SINS initial alignment. As previously mentioned, this filter uses the past, current and future measurement information in its estimation procedure so the GPIDF approach can improve the accuracy of the SINS alignment process. Furthermore, regarding the integral part used in the GPIDF, this filter has desirable robustness property compared to the standard KF. Therefore, the GPIDF alignment approach can increase the performance of the alignment process in the presence of large misalignment angles uncertainty. The block diagram of the GPIDF alignment scheme is shown in Figure 1. The measurement input of the GPID filter is the difference between the velocity vector calculated from INS algorithm and the exact velocity vector in the inertial frame. During the alignment phase, the estimated errors are fed back to the aligning SINS to correct the transformation matrix. Similar to all closed-loop self-alignment methods, the velocity and misalignment errors computed from GPID filter are reset to zero when the correction feedback term is applied to the SINS.

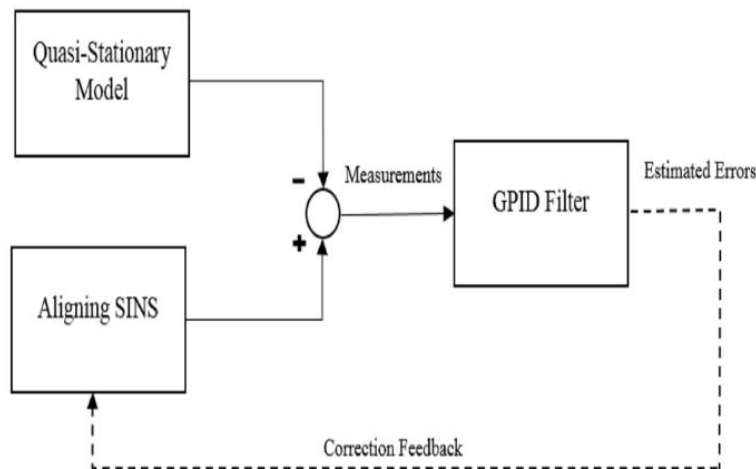


Figure 1. The block diagram of the GPIDF alignment scheme

In the GPIDF alignment approach it is also necessary to reset the integral and derivative parts of estimation ( $\mathbf{x}_I$  and  $\mathbf{x}_D$ ) to zero when the feedback term is applied. In conventional Kalman filter alignment methods, the correction and the measurement update are usually performed at the same rate (1 Hz). Considering that the GPIDF parameters reset once the correction feedback is applied



and in order to benefit from the integral and derivative parts of the GPID filter, the correction term must be applied at a lower rate in comparison to measurement update rate of the GPIDF. Otherwise, the proposed GPIDF alignment approach would perform similar to the standard KF-based method.

#### IV. EXPERIMENTAL TEST RESULTS

##### a. Initial setups and test description

In this section, experimental turntable test is performed to evaluate the performance of the proposed GPIDF alignment approach under simulated marine mooring condition. The three-axis turntable and the technical-grade Inertial Measurement Unit (IMU) implemented in this test are shown in Figure 2. The IMU is developed by Shiraz University and it consists of three fiber-optic gyroscopes and three quartz accelerometers. The technical specifications of the IMU's inertial sensors and the turntable are shown in Table 1. and Table 2., respectively. The axes of the IMU are accurately aligned with respect to the axes of the turntable. So, the inner, middle and outer frames generate vessel's roll, pitch, and yaw motions, respectively. The outputs of the inertial sensors and the angles information of the turntable are synchronized and recorded for post processing.

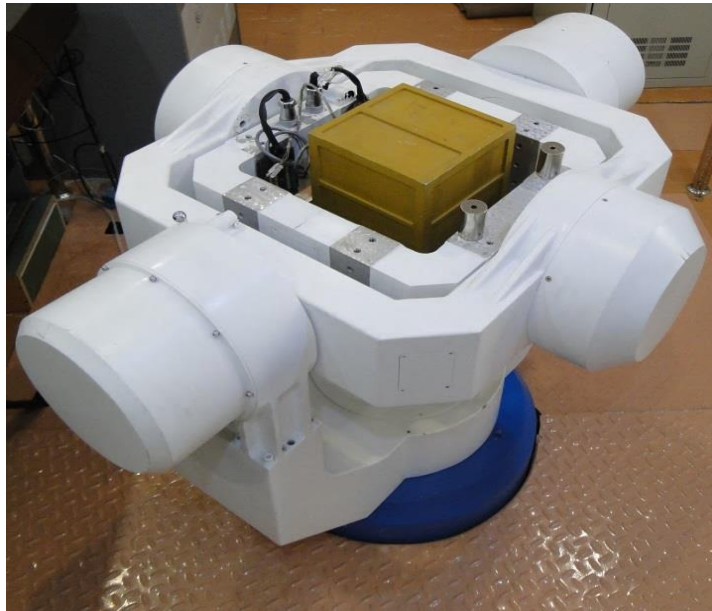


Figure 2. The three-axis turntable and the IMU

Table 1. Technical specification of IMU's inertial sensors

Gyroscope Bias Drift	0.01 deg / hr
Gyroscope Angular Random Walk	0.001 deg / $\sqrt{\text{hr}}$
Accelerometer Constant Bias	$\pm 50 \mu\text{g}$
Accelerometer Velocity Random Walk	0.03 $m/s/\sqrt{\text{hr}}$

Table 2. Specification of the three-axis turntable

Parameter	Precision
Position resolution	$\pm 5''$ (0.001 deg)
Position range	$\pm 360^\circ$
Angular rate range	$\pm 400 \text{ deg} / \text{s}$
Angular rate resolution	0.0001 $\text{deg} / \text{hr}$

To assess the alignment accuracy and rapidness of a marine SINS product, the European standard for marine gyro-compasses has proposed a test which is named, Settling Time Scorsby Table Test (Scorsby test) [26]. This test is chosen to evaluate the performance of the proposed GPIDF alignment in our experimental turntable test. The swinging parameters are chosen based on the Scorsby test procedure which is shown in Table 3.

Table 3. The swinging parameters of the Scorsby test

	Amplitude ( $^\circ$ )	Period (s)	Swing Center( $^\circ$ )
Inner	5	15	0
Middle	5	6	0
Outer	0	0	315

b. The Scorsby test results

In order to show the performance of the proposed alignment method, the test results of the GPIDF approach are compared with the standard Kalman filter based alignment method. To have a fair comparison sight, all filtering parameters such as  $\mathbf{Q}$ ,  $\mathbf{R}$ ,  $\mathbf{P}_0$  and  $\bar{\mathbf{x}}_0$  are also considered identical for both of the alignment approaches as follows:

$$\bar{\mathbf{x}}_0 = \mathbf{0}_{6 \times 1}$$

$$\mathbf{P}_0 = \text{diag} [ (0.1 \text{ m/s})^2, (0.1 \text{ m/s})^2, (0.1 \text{ m/s})^2, \\ (1^\circ)^2, (1^\circ)^2, (10)^\circ, (0.05\text{mg})^2, (0.05\text{mg})^2, (0.05\text{mg})^2, \\ (.01^\circ/\text{hr})^2, (0.01^\circ/\text{hr})^2, (0.01^\circ/\text{hr})^2 ]$$

$$\mathbf{R} = \text{diag} [ (0.01 \text{ m/s})^2, (0.01 \text{ m/s})^2, (0.01 \text{ m/s})^2 ]$$

$$\mathbf{Q} = \text{diag} [ (0.06 \text{ m/s}/\sqrt{\text{hr}})^2, (0.06 \text{ m/s}/\sqrt{\text{hr}})^2, (0.06 \text{ m/s}/\sqrt{\text{hr}})^2, \\ (0.008 \text{ deg}/\sqrt{\text{hr}})^2, (0.008 \text{ deg}/\sqrt{\text{hr}})^2, (0.008 \text{ deg}/\sqrt{\text{hr}})^2, \\ 0, 0, 0, 0, 0, 0 ]$$

The initial azimuth angle is considered appropriately (280 degrees) in both alignment approaches which causes to have a large initial azimuth angle at the beginning of alignment process. The Scorsby test is performed for 900 seconds. By considering  $\mathbf{K}_1 = k_i * \mathbf{K}_p$  and  $\mathbf{K}_1 = k_d * \mathbf{K}_p$  in (16) and (17), the proportional-integral type of the GPIDF is implemented in this test ( $k_i = 1$  and  $k_d = 0$ ). The estimated yaw angle and the components of the residual error vector ( $\mathbf{y}(k) - \mathbf{C}\hat{\mathbf{x}}(k|k)$ ) are shown in Figure 3 to Figure 6.

Mohammad Ali Rahgoshay, Paknoosh Karimaghaie, Fereidoon Shabaninia  
INITIAL ALIGNMENT OF FIBER-OPTIC INERTIAL NAVIGATION SYSTEM WITH LARGE  
MISALIGNMENT ANGLES BASED ON GENERALIZED PROPORTIONAL-INTEGRAL-DERIVATIVE  
FILTER

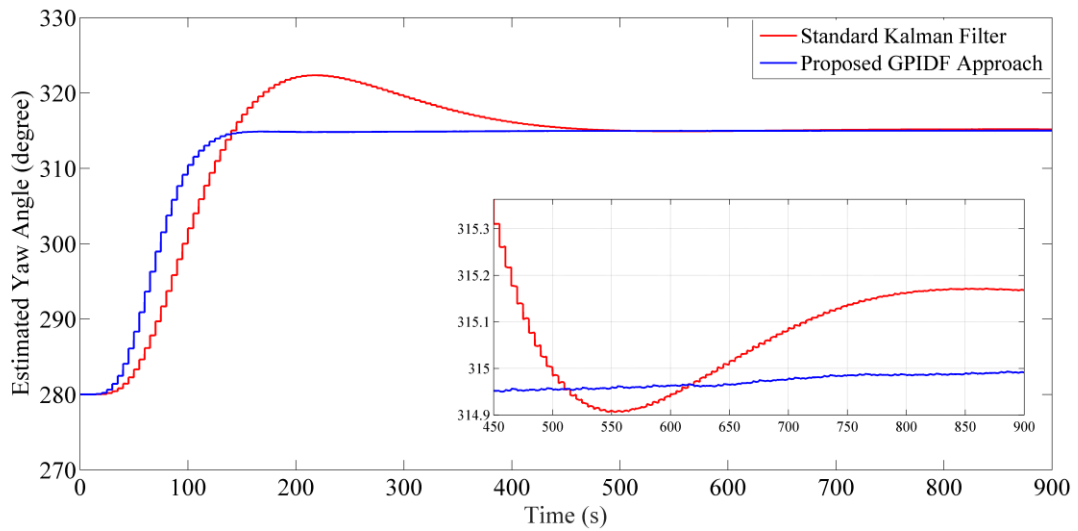


Figure 3. The estimated yaw angle

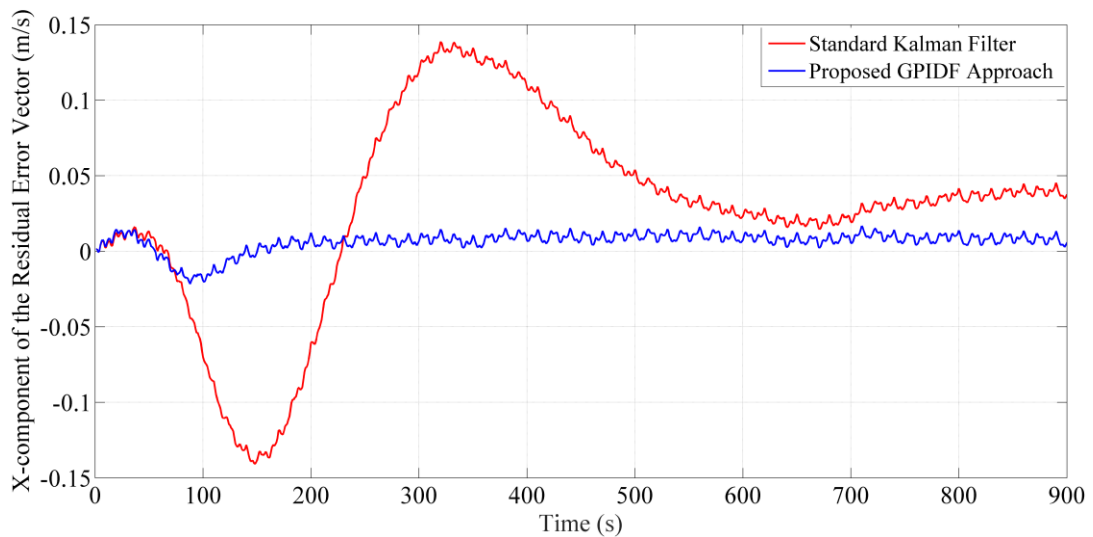


Figure 4. The X-component of the residual error vector

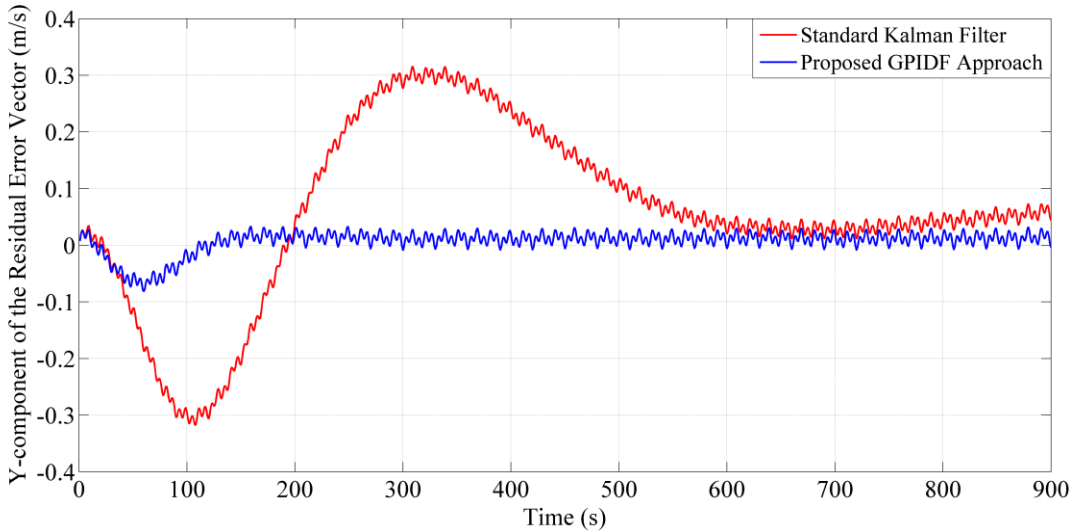


Figure 5. The Y-component of the residual error vector

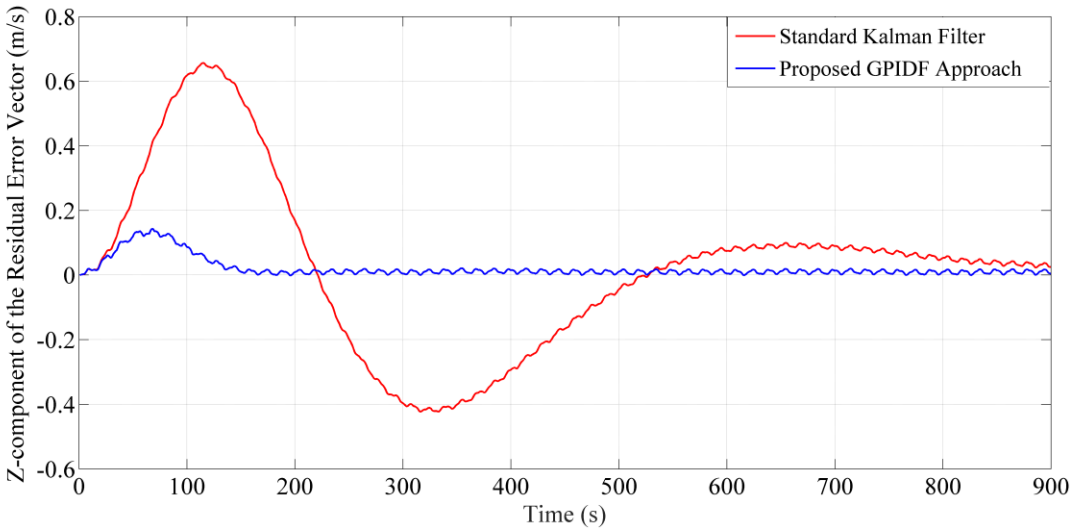


Figure 6. The Z-component of the residual error vector

The test results show that unlike the standard KF-based alignment, the proposed GPIDF alignment approach has superior performance in the presence of the large misalignment angles uncertainty. In fact, due to the existence of initial large azimuth (yaw) angle, the linear error model of SINS used in standard Kalman filter does not accurately describe actual nonlinear dynamics error of SINS and consequently, the KF is not an optimal solution for this alignment problem. Resulting from the integral part which utilized in the proposed GPIDF alignment approach, this method has a desirable robustness property. Therefore, the proposed alignment approach outperforms the standard KF alignment in the presence of large misalignment angles model uncertainty without implementing the nonlinear error model of SINS. As it is clear from Figure 3 to Figure 6, the residual error convergence speed is greatly improved in the proposed GPIDF alignment approach so the estimated azimuth angle rapidly converges to the desirable value compared to standard KF-based alignment method.

The estimated yaw RMS error and its standard deviation are shown in Table 4 for 600 seconds of the test. The statistics demonstrate that the proposed GPIDF alignment approach has a more accurate and rapid estimation compared to the standard KF-based alignment method and achieves desirable accuracy in 400 seconds.

Table 4. The statistics for estimated yaw RMS error in the Scorsby test

	<b>Yaw Error (°)</b>	<b>0-200 (s)</b>	<b>200-400 (s)</b>	<b>400-600 (s)</b>
<b>Standard Kalman Filter</b>	RMS	21.6066	5.0096	0.3723
	Std	15.8784	2.1165	0.3321
<b>Proposed GPIDF Approach</b>	RMS	18.8104	0.1510	0.0476
	Std	13.8810	0.0372	0.0078

## VI. CONCLUSIONS

A novel robust alignment approach based on generalized proportional-integral-derivative filter is proposed in this article. This new approach has superior performance compared to the conventional standard Kalman filter based alignment method. By using the significant advantages of the GPID filter, the proposed alignment method has desirable performance in the presence of large initial misalignment angles uncertainty. The experimental turntable test results confirm the validity and efficiency of the proposed alignment approach.

## REFERENCES

- [1] D. Titterton and J. L. Weston, Strapdown inertial navigation technology vol. 17: IET, 2004.
- [2] D. Simon, Optimal state estimation: Kalman, H infinity, and nonlinear approaches: John Wiley & Sons, 2006.
- [3] D. Simon, "Kalman filtering with state constraints: a survey of linear and nonlinear algorithms," IET Control Theory & Applications, vol. 4, pp. 1303-1318, 2010.
- [4] L. Zhang, H. Yang, S. Zhang, H. Cai, and S. Qian, "Kalman filtering for relative spacecraft attitude and position estimation: a revisit," Journal of Guidance, Control, and Dynamics, vol. 37, pp. 1706-1711, 2014.
- [5] Botero V., J.S., Hernandez, W.: Orientation of a triaxial accelerometer using a homogeneous transformation matrix and Kalman filters", International Journal on Smart Sensing and Intelligent Systems, vol. 7, no. 4, pp. 1631–1646, 2014.
- [6] G. P. Pappas, M. A. Zohdy, "Extended Kalman filtering and pathloss modeling for shadow power parameter estimation in mobile wireless communications", International Journal on Smart Sensing and Intelligent Systems, vol. 7, no. 2, pp. 898-924, 2014.
- [7] V. Ramchandani, K. Pamarthi, S. R. Chowdhury, "Comparative Study of Maximum Power Point Tracking using Linear Kalman Filter & Unscented Kalman Filter for Solar Photovoltaic Array on Field Programmable Gate Array", International Journal on Smart Sensing and Intelligent Systems, vol.5, no.3, pp.701-716, 2012.

- [8] L. Chang, J. Li, and S. Chen, "Initial alignment by attitude estimation for strapdown inertial navigation systems," *IEEE Transactions on Instrumentation and Measurement*, vol. 64, pp. 784-794, 2015.
- [9] H. Li, Q. Pan, X. Wang, X. Jiang, and L. Deng, "Kalman Filter Design for Initial Precision Alignment of a Strapdown Inertial Navigation System on a Rocking Base," *Journal of Navigation*, vol. 68, pp. 184-195, 2015.
- [10] R. Tomari, Y. Kobayashi, and Y. Kuno, "Socially acceptable smart wheelchair navigation from head orientation observation," *International Journal on Smart Sensing & Intelligent Systems*, vol. 7, pp. 630-643, 2014.
- [11] J. A. Hesch, D. G. Kottas, S. L. Bowman, and S. I. Roumeliotis, "Consistency analysis and improvement of vision-aided inertial navigation," *IEEE Transactions on Robotics*, vol. 30, pp. 158-176, 2014.
- [12] D. Gu, N. El-Sheimy, T. Hassan, and Z. Syed, "Coarse alignment for marine SINS using gravity in the inertial frame as a reference," in *2008 IEEE/ION Position, Location and Navigation Symposium*, pp. 961-965, 2008.
- [13] W. Gao, Y. Che, X. Zhang, J. Feng, and B. Zhang, "A fast alignment algorithm based on inertial frame for marine SINS," in *2012 IEEE International Conference on Mechatronics and Automation*, pp. 1756-1760, 2012.
- [14] D. Yuan, X. Ma, Y. Liu, C. Hao, and Y. Zhu, "Dynamic initial coarse alignment of SINS for AUV using the velocity loci and pressure sensor," *IET Science, Measurement & Technology*, vol. 10, pp. 926-933, 2016.
- [15] W. Li, J. Wang, L. Lu, and W. Wu, "A novel scheme for DVL-aided SINS in-motion alignment using UKF techniques," *Sensors*, vol. 13, pp. 1046-1063, 2013.
- [16] P. G. Savage, "Moving Base INS Alignment with Large Initial Heading Error," *Strapdown Associates, Inc.: Maple Plain, MN, USA*, 2014.
- [17] H. Hong, J. Lee, and C. Park, "Performance improvement of in-flight alignment for autonomous vehicle under large initial heading error," *IEE Proceedings-Radar, Sonar and Navigation*, vol. 151, pp. 57-62, 2004.
- [18] R. M. Rogers, "IMU In-Motion Alignment Without Benefit of Attitude Initialization," *Navigation*, vol. 44, pp. 301-311, 1997.



- [19] J. Sun, X.-S. Xu, Y.-T. Liu, T. Zhang, and Y. Li, "Initial alignment of large azimuth misalignment angles in SINS based on adaptive UPF," *Sensors*, vol. 15, pp. 21807-21823, 2015.
- [20] J. Li, N. Song, G. Yang, and R. Jiang, "Fuzzy adaptive strong tracking scaled unscented Kalman filter for initial alignment of large misalignment angles," *Review of Scientific Instruments*, vol. 87, p. 075118, 2016.
- [21] L. Zhang, C. Yang, Q. Chen, and F. Yan, "Robust H-infinity CKF/KF hybrid filtering method for SINS alignment," *IET Science, Measurement & Technology*, vol. 10, pp. 916-925, 2016.
- [22] J. Ali and M. Ushaq, "A consistent and robust Kalman filter design for in-motion alignment of inertial navigation system," *Measurement*, vol. 42, pp. 577-582, 2009.
- [23] S. P. Dmitriyev, O. A. Stepanov, and S. V. Shepel, "Nonlinear filtering methods application in INS alignment," *IEEE Transactions on Aerospace and Electronic Systems*, vol. 33, pp. 260-272, 1997.
- [24] J. Zhang, X. He, and D. Zhou, "Generalised proportional–integral–derivative filter," *IET Control Theory & Applications*, vol. 10, pp. 2339-2347, 2016.
- [25] F. Sun, H. Lan, C. Yu, N. El-Sheimy, G. Zhou, T. Cao, et al., "A robust self-alignment method for ship's strapdown INS under mooring conditions," *Sensors*, vol. 13, pp. 8103-8139, 2013.
- [26] L. Constantin and J. Kieffer, "OCTANS 1 MO(ISO 8728) certification tests at the LRBA," in *Symposium Gyro Technology 2000*, Stuttgart, Germany, p. 17, 2000.